Original Article

JCBFM

Journal of Cerebral Blood Flow & Metabolism
2016, Vol. 36(12) 2108–2121

DOI: 10.1177/0271678X16642233
jcbfm.sagepub.com

SAGE

Blood–brain barrier breakdown promotes macrophage infiltration and cognitive impairment in leptin receptor-deficient mice

Alexis M Stranahan[1], Shuai Hao[1], Aditi Dey[1], Xiaolin Yu[1] and Babak Baban[2,3]

Abstract

Accumulating evidence indicates that obesity accelerates the onset of cognitive decline. While mechanisms are still being identified, obesity promotes peripheral inflammation and increases blood–brain barrier (BBB) permeability. However, no studies have manipulated vascular permeability in obesity to determine whether BBB breakdown underlies memory deficits. Protein kinase Cβ (PKCβ) activation destabilizes the BBB, and we used a PKCβ inhibitor (Enzastaurin) to block BBB leakiness in leptin receptor-deficient (db/db) mice. Enzastaurin reversed BBB breakdown in db/db mice and normalized hippocampal function without affecting obesity or metabolism. Flow cytometric analysis of forebrain mononuclear cells (FMCs) from db/db mice revealed macrophage infiltration and induction of the activation marker MHCII in microglia and macrophages. Enzastaurin eliminated macrophage infiltration and MHCII induction, and protein array profiling revealed parallel reductions in IL1β, IL6, MCP1, and TNFα. To investigate whether these signals attract peripheral monocytes, FMCs from Wt and db/db mice were plated below migration inserts containing peritoneal macrophages. Peritoneal macrophages from db/db mice exhibit increases in transmigration that were blocked by recombinant IL1RA. These studies indicate that BBB breakdown impairs cognition in obesity and diabetes by allowing macrophage infiltration, with a potential role for IL1β in trafficking of peripheral monocytes into the brain.

Keywords

Diabetes, obesity, inflammation, microglia, learning and memory, hippocampus

Received 20 November 2015; Revised 2 March 2016; Accepted 7 March 2016

Introduction

Chronic inflammation in obesity is most recognized for its role in the development of metabolic and cardiovascular disease,[1] but increasing evidence suggests that inflammation also impacts the central nervous system.[2,3] Inflammation in hypothalamic nuclei has been widely reported in models of metabolic dysfunction,[2] but neuroinflammation also occurs outside of circuits directly implicated in food intake and energy expenditure.[3–6] Hippocampal neurons are required for associational memory and exhibit early vulnerability during progression from amnestic mild cognitive impairment to dementia, including Alzheimer's disease (AD).[7,8] Cross-sectional and longitudinal studies suggest that obesity and diabetes each independently increase AD risk,[8–15] but the cellular mechanisms for susceptibility to dementia in these conditions have yet to be identified.

The blood–brain barrier (BBB) is a source of passive and active protection for cells residing in the brain parenchyma.[16,17] Tight junctions between endothelial cells

[1]Department of Neuroscience and Regenerative Medicine, Medical College of Georgia, Georgia Regents University, Augusta, GA, USA
[2]Department of Oral Biology, Medical College of Georgia, Georgia Regents University Augusta, GA, USA
[3]Plastic Surgery Section, Department of Surgery Medical College of Georgia, Georgia Regents University, Augusta, GA, USA

Corresponding author:
Alexis M Stranahan, Department of Neuroscience and Regenerative Medicine, Medical College of Georgia, Georgia Regents University, 1120 15th St, CA3009, Augusta, GA 30912, USA.
Email: astranahan@gru.edu

restrict diffusion to gases and lipid-soluble steroids, with most transport occurring via receptor-mediated transcytosis.[18] However, the notion of an impenetrable barrier is being eroded by demonstrations of increased BBB permeability in multiple disease states, including obesity, aging, and Alzheimer's disease.[19–21] These findings have led to reinterpretation that the BBB is as less of a barrier and more of a gate, with dynamic regulation of gating by circulating factors and local signals from neurons and glia. In acute injuries, such as traumatic brain injury and ischemic stroke, there is consensus that cerebrovascular disruption elicits secondary injury by exposing the brain to circulating factors.[22] In chronic conditions such as obesity and diabetes, the mechanisms that initiate and perpetuate BBB breakdown have yet to be identified, and the consequences for synaptic function remain poorly understood. Peripheral inflammation increases BBB permeability, but also influences cells of the central nervous system (CNS) via BBB-independent mechanisms.[23] Obesity increases inflammatory cytokines in multiple brain regions, including the hippocampus,[4–6] but there has been no investigation into whether these effects are mediated by, or independent of, BBB leakiness.

Microglia are brain-resident phagocytes that constantly monitor the neuropil with motile processes for detection and clearance of cellular debris.[24] Peripheral macrophages and microglia arise from a common embryonic precursor, but diverge thereafter, with minimal macrophage penetrance across the BBB under normal conditions.[25] Activation of protein kinase Cβ (PKCβ) increases BBB permeability and allows bone marrow-derived immune cells to enter the nervous system in models of infectious disease.[26] Diabetes also promotes PKCβ-mediated cerebrovascular breakdown in the retina,[27] but mechanisms for BBB breakdown in the CNS remain to be determined, and the reported relationships between BBB breakdown, microglial activation, and cognitive deficits remain correlative at present.[4,5,28]

We used the selective PKCβ inhibitor LY-317615 (Enzastaurin) to re-seal the BBB in mice with genetic diabetes and obesity (db/db mice). This approach reversed BBB leakiness based on cellular and functional measures and normalized hippocampal synaptic plasticity. Reinstatement of BBB integrity prevented macrophage infiltration into the brain parenchyma and blocked induction of inflammatory cytokines in forebrain mononuclear cells from db/db mice. Analysis of transmigration revealed greater attraction between peritoneal macrophages and forebrain mononuclear cells from db/db mice. Increases in migration were dependent on interleukin 1 signaling, suggesting that BBB breakdown enables IL1-mediated macrophage infiltration and cognitive dysfunction in diabetes and obesity.

Materials and methods

Animals and drug treatments

Male leptin receptor mutant (db/db) mice and C57Bl6J (Wt) mice were purchased from Jackson Laboratories (Bar Harbor, Maine) at six weeks of age. After two-week acclimation, db/db mice were randomly assigned to receive vehicle (0.5% methyl cellulose; db/Veh) or the protein kinase Cβ (PKCβ) inhibitor Enzastaurin (Cayman Chemical, Ann Arbor, MI, USA; db/Enz). Enzastaurin was administered at 50 mg/kg daily by gavage for two weeks. Wildtype (Wt) mice received vehicle throughout the treatment period (Wt/Veh). Because Enzastaurin reduced body weight in Wt mice to less than 20% of Wt/Veh after two weeks, subsequent experiments excluded this treatment condition. For all groups of mice, body weights were measured weekly, and food intake data were collected on two successive days per week. In a subset of mice, glycemic control was assessed with intraperitoneal glucose tolerance testing, as described.[29] All of the animal procedures used in these studies were approved by the Institutional Animal Care and Use Committee of Georgia Regents University and followed the NIH *Guide for the Care and Use of Laboratory Animals*, and the manuscript adheres to the ARRIVE (Animal Research: Reporting in Vivo Experiments) guidelines for reporting animal experiments.

Fluorescein penetration assay

For assessment of BBB integrity, mice were injected with sodium fluorescein (NaFl; 10 mg/kg, IP; $n = 6–8$). Forty-five minutes after NaFl injection, mice were euthanized by transcardial perfusion with saline under Isoflurane anesthetic. One hemisphere was excised and fixed in 4% paraformaldehyde (PFA) for visualization of NaFl penetrance in brain sections. The hippocampus and cortex were excised from the opposite hemisphere and frozen for extraction and fluorometric quantification on a Biotek plate reader (Biotek, VT, USA). The extraction and quantification procedures were carried out in a blind manner. Fluorescence emission values from duplicate wells containing brain extracts were fit to a standard curve, averaged, and expressed relative to total protein as determined by Bradford assay. For the fixed hemisphere, brains were sectioned at 40 microns using a Vibratome (Leica, Buffalo Grove, IL, USA) under low-light conditions. After quenching autofluorescence in 1% sodium borohydride, sections were reacted with a polyclonal antibody against NaFl (Vector Labs, Burlingame, CA, USA). The primary antibody was amplified using Alexa 488-conjugated secondary antibodies and sections were counterstained with DAPI for imaging. Montage images of NaFl

labeling in hippocampal sections were acquired through the 10× objective on a Zeiss MTB upright fluorescence microscopy with the aid of Microlucida software (Microbrightfield, Williston, VT, USA).

Behavioral testing

Groups of ($n = 9$–11) mice from each cohort were tested in the Y-maze and novel object preference tests. Testing in both paradigms was carried out between 18:00 and 22:00 h (lights-off at 1800) under red light illumination, as described.[4,5,30] Testing in the Y-maze involved (6) left/right choices, with correct choices expressed relative to the total number of potential alternations. Novel object recognition testing involved 10-min exposure to two identical objects, followed by 30 min in the home cage, after which the mouse was returned to the arena in the presence of one novel and one familiar object. After 5 min of object exploration, the mouse returned to the home cage for 1.5 h before re-exposure to the familiar object and a different novel object. Test sessions were captured on video and analyzed offline at half speed by an observer blinded to the treatment conditions. The duration of each exploratory interval was recorded and expressed relative to the total amount of object exploration (novel + familiar) for each trial.

Hippocampal slice preparation and electrophysiology

Hippocampal slice preparation and extracellular recording followed previously published methods.[4,5,30,31] Acute slices were cut on a Vibratome (Leica, Buffalo Grove, IL, USA) into a bath of oxygenated artificial cerebrospinal fluid (ACSF). After 1 h recovery at 37°C, extracellular recordings were performed in ACSF in the presence of 50 μM picrotoxin (Sigma-Aldrich, St. Louis, MO, USA). For some experiments, Enzastaurin (1 μM)[32] was bath-applied for 30 min before and during the recordings. Electrodes were positioned in the middle molecular layer superficial to the dentate gyrus, and medial perforant path inputs were functionally identified by the presence of paired-pulse depression (PPD).[33] PPD magnitude was determined using interpulse intervals of 50, 200, 500, and 1000 ms, and quantified by expressing the slope of the second (S2) field excitatory postsynaptic potential (fEPSP) relative to the first fEPSP (S1). The baseline stimulation intensity was set at 50% of maximal fEPSP slope generated from the input/output curve. Stimuli were delivered at 0.05 Hz for baseline and post-tetanus recording, and LTP was induced with a single train (1 s, 100 Hz). Data were collected using pClamp version 10.3.4 and analyzed in Clampfit by an experimenter blind to treatment condition (Molecular Devices, Sunnyvale, CA, USA). The n-sizes for electrophysiological recordings reflect the number of slice preparations, with ($n = 12$–16) slices from ($n = 9$–11) mice in each condition.

Forebrain mononuclear cell isolation and flow cytometry

Forebrain mononuclear cells (FMCs) were isolated from adult mice according to previously published protocols.[4,5,29] In brief, groups of ($n = 8$) mice from each condition were transcardially perfused with saline under Isoflurane anesthetic. The brain was removed and the cerebellum was excised and discarded before preparation of cell suspensions by manual homogenization. Forebrain mononuclear cells were separated by centrifugation on a discontinuous gradient of isoosmotic Percoll. The 70%/35% interface was collected and washed in Dulbecco's phosphate-buffered saline (dPBS) before determination of viability and yield using the ViaCount assay on a Guava EasyCyte 5 flow cytometer (Millipore, Temecula, CA, USA).

For flow cytometry, cells in suspension (5×10^4 cells/100 μL) were blocked in 1 × dPBS containing 10% heat-inactivated fetal bovine serum (dPBS + FBS) for 30 min before incubation with a phycoerythrin-Cy5 (PE-Cy5)-conjugated antibody against CD45 and FITC-conjugated antibodies against CD11b, major histocompatibility complex II (MHCII), or Ly6C (all antibodies from AbD Serotec). After primary antibody incubation, cells were pelleted by centrifugation and resuspended in 1 × dPBS + FBS containing the dead cell marker Sytox Orange (1:1000; Invitrogen, Carlsbad, CA, USA). After 10 min of incubation with Sytox Orange, cells were centrifuged and resuspended in 500 μL 1 × dPBS for flow cytometry.

Thresholds for acquisition were determined using isotype controls and compensation parameters were generated from single-channel acquisition of PE-Cy5, PE, and FITC-conjugated antibodies or stains. For each label or combination of labels, 1×10^4 events were acquired on a Guava EasyCyte 5 flow cytometer (Millipore). Cells were gated on forward and side scatter and Sytox Orange-positive cells were excluded. The proportion of cells expressing different antigens was determined using InCyte software (Millipore).

Peritoneal macrophage collection

Peritoneal macrophages were collected from unstimulated wildtype and db/db mice by lavage, as described.[34] In brief, mice were housed under pathogen-free conditions before being deeply anesthetized with Isofluorane for cell collection. The abdominal wall was cleaned with Nolvasan (Fisher Scientific) and a 1–2 cm incision was made through the skin and

peritoneal muscle just below the xyphoid process. The muscle layer was lifted with forceps to create a pocket and 5 mL of cold dPBS was injected through a blunt 18 g needle. The fluid was then withdrawn and transferred to a 15 mL tube before repeating the procedure to collect approximately 5 mL from each animal. Tubes containing peritoneal fluid were then centrifuged at $400 \times g$ (4°C) for 10 min to pellet cells before resuspension in DMEM. An aliquot from each preparation was used to determine yield using the ViaCount assay on a Guava flow cytometer as described above. The majority (>90%) of cells collected using this approach were SSClow/CD11b+/CD45+ macrophages based on flow cytometric analysis.

Migration assays

For analysis of transmigration, FMCs isolated from ($n = 8$–11) mice in each condition were plated on coverslip-bottom 24-well plates in serum-free DMEM (1×10^4 cells/well). After 2-h adherence, the plating medium was exchanged for maintenance medium (DMEM with 5%FBS). Boyden chamber inserts (8 micron pore size; Cell Biolabs, San Diego, CA, USA) containing peritoneal macrophages in serum-free media (1×10^5) were suspended above each well in contact with the FMC maintenance media. Since FBS itself is an attractant, control wells with macrophages suspended above DMEM + 5%FBS were run for each experiment (Supplementary Figure 1A). Additional control wells containing macrophages suspended above serum-free DMEM were included to examine whether macrophages from db/db mice exhibit greater transmigration in the absence of an attractant (Supplementary Figure 1B). The final set of control wells involved plating FMCs below inserts containing only serum-free DMEM to examine the possibility that plated FMCs might detach and adhere to the bottom of the insert (Supplementary Figure 1C).

For some experiments, Enzastaurin (1 μM),[32] recombinant interleukin 1 receptor antagonist (IL1RA, 10 μg/mL[35]; Sobi Inc., Stockholm, Sweden) or MCP1 receptor antagonist (RS504393, 350 nM[36]; Tocris Bioscience) was added to the macrophages in the upper chamber. In other experiments, antibodies were added to FMCs in the lower well to neutralize or inhibit interleukin 6 (0.5 μg/mL[37]; R&D Systems Minneapolis, MN, USA) or TNFα (15 μg/mL[38]; Abbott Laboratories, Chicago, IL, USA). Plates and inserts were incubated overnight at 37°C under 5% CO_2.

The next day, inserts were either fixed in 4% paraformaldehyde (PFA) or moved into a fresh well containing detachment media according to the manufacturer's instructions. FMCs plated below the inserts were also either fixed in PFA or detached and lysed using reagents from the migration assay kit (Cell Biolabs, San Diego, CA, USA). Protein lysates were stained with Cyquant Green according to the manufacturer's instructions and transferred to duplicate wells of a 96-well plate for quantification on a fluorescent plate reader (Biotek). Fixed inserts were stained with DAPI and imaged through a 10× objective on a Zeiss MTB epifluorescence microscope.

Protein arrays and western blotting

To generate conditioned media for protein array profiling, 1×10^5 FMCs were isolated from ($n = 6$) mice in each condition and plated on glass coverslips in DMEM containing 0.5% heat-inactivated fetal bovine serum (Gibco). After 2 h of adherence in plating medium at 37°C under 5% CO_2, cells were switched to serum-free media for an additional 2 h before collection and storage of conditioned media at −80°C. The cells were then detached by gentle titration with dPBS before being transferred to tubes and lysed for protein extraction according to standard protocols.[4,5] Conditioned media samples were applied to chemiluminescent protein array membranes and detected according to the manufacturer's instructions (R&D Systems) before visualization on a Protein Simple digital imaging system.

Protein extraction and quantification of total protein by Bradford assay took place as described.[4,5] In brief, hippocampal protein extracts (50 μg) or FMC protein lysates (20 μg) were loaded and separated through gel electrophoresis. Proteins were transferred to nitrocellulose membranes, blocked in 5% nonfat milk, and probed with antibodies against claudin 5 (Abcam, Cambridge, MA, USA), occludin (Abcam, Cambridge, MA, USA), and β-actin (Sigma-Aldrich, St. Louis, MO, USA). For cell lysates, membranes were blocked in 5% bovine serum albumin before being probed with antibodies against IL1β, IL6, MCP1, and TNFa (all antibodies from Cell Signaling Technologies, Danvers, MA, USA). Primary antibodies were applied at 1:1000 overnight at 4°C and detected with HRP-conjugated secondary antibodies directed against the appropriate species. Bands were visualized on a Protein Simple chemiluminescence imager and band intensities were quantified in ImageJ.

Statistics

Body weights, fat pad weights, and food intake data were compared across conditions using one-way ANOVA. Data from glucose tolerance testing and from the novel object recognition task were analyzed using one-way repeated measures ANOVA. Western blot endpoints were analyzed using one-way ANOVA,

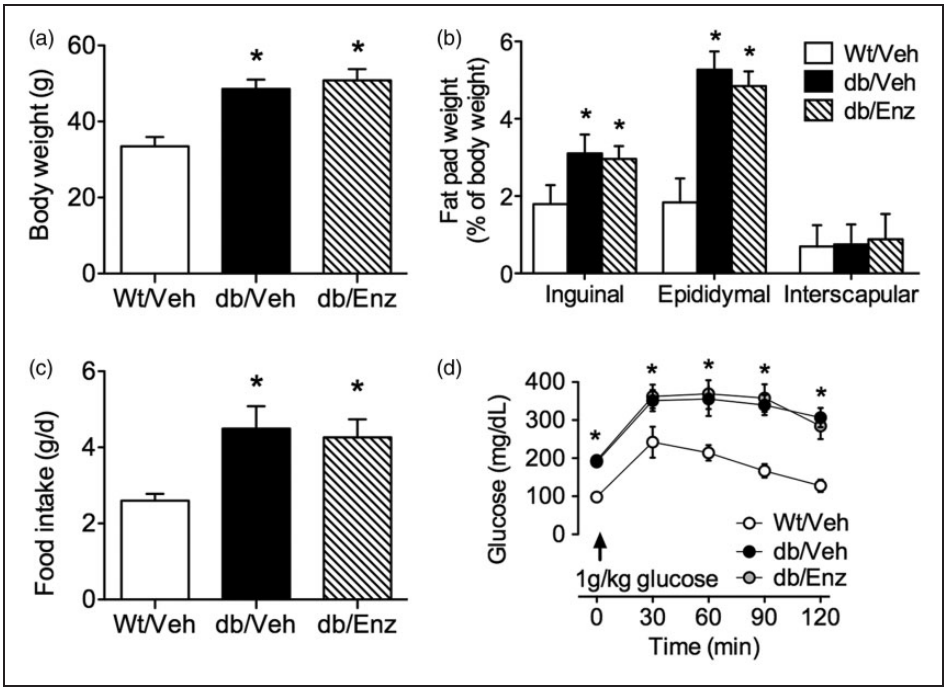

Figure 1. Oral administration of the blood–brain barrier sealing compound Enzastaurin does not impact food intake, obesity, or adiposity in leptin receptor-deficient mice. (a) Treatment with Enzastaurin, a PKCβ inhibitor previously shown to prevent BBB leakiness in models of infectious disease,[26] does not cause weight loss in db/db mice when administered daily during the final two weeks of the study (db/Enz; 50 mg/kg/d, PO). Vehicle-treated db/db and Wt mice received daily oral administration of 0.5% methyl cellulose (db/Veh, Wt/Veh). (b) Enzastaurin administration had no effect on food intake during the two-week treatment period. (c) db/db mice reliably exhibit greater adiposity, based on increased weights of individual fat depots relative to body weight. The magnitude of this effect was unchanged by Enzastaurin treatment. (d) The severity of insulin resistance in db/db mice was unaffected by systemic Enzastaurin administration. For all graphs, bars or symbols depict the mean of ($n = 10$) mice in each group. Error bars represent the SEM and asterisks (*) denote statistical significance at $p < 0.05$ following one-way ANOVA (a, b, c) or repeated measures one-way ANOVA (d) with Bonferonni's post hoc.

as were the electrophysiological and flow cytometry data, and data from the transmigration assays. All ANOVA designs used $p < 0.05$ as the threshold for statistical significance and were followed by *post hoc* comparisons using Bonferroni-corrected *t*-tests. Analyses were carried out in Graphpad Prism version 5.0 (La Jolla, CA, USA).

Results

No effect of PKCβ antagonism on body weight or food intake in db/db mice

db/db mice exhibit severe obesity and insulin resistance beginning at five weeks of age.[39] Treatment with the PKCβ inhibitor Enzastaurin did not affect body weight in db/db mice when administered daily for two weeks beginning at eight weeks old (db/Enz; 50/mg/kg/d, PO; $F_{2,27} = 12.87$, $p < 0.01$; Figure 1(a)). Consistent with the reductions in body weight reported following administration of ruboxistaurin, a related PKCβ inhibitor,[40] Enzastaurin reduced weight gain in Wt mice (two-week weight gain, grams; mean ± SEM, Wt/Veh = 6.5 ± 1.1, Wt/Enz = 2.2 ± 0.9). Because Enzastaurin reduced body weights beyond inclusion criteria in Wt mice, subsequent experiments did not include this treatment condition. Enzastaurin did not alter adiposity in db/db mice, as the weights of the inguinal, epididymal, and interscapular fat pads were comparable in db/Enz and vehicle-treated db/db mice (db/Veh), relative to vehicle-treated wildtype mice (Wt/Veh; Figure 1(b)). Both db/Enz and db/Veh mice exhibited similar hyperphagia relative to Wt/Veh mice ($F_{2,27} = 10.14$, $p < 0.01$; Figure 1(c)), and the severity of insulin resistance was unaffected by PKCβ antagonism (Figure 1(d)). These measures indicate that PKCβ antagonism does not influence the development of obesity and diabetes in db/db mice.

PKCβ-mediated blood–brain barrier breakdown in genetic obesity

We next examined the effects of PKCβ antagonism on BBB integrity. Fluorescein penetrance into the neuropil was evident on hippocampal sections from db/Veh

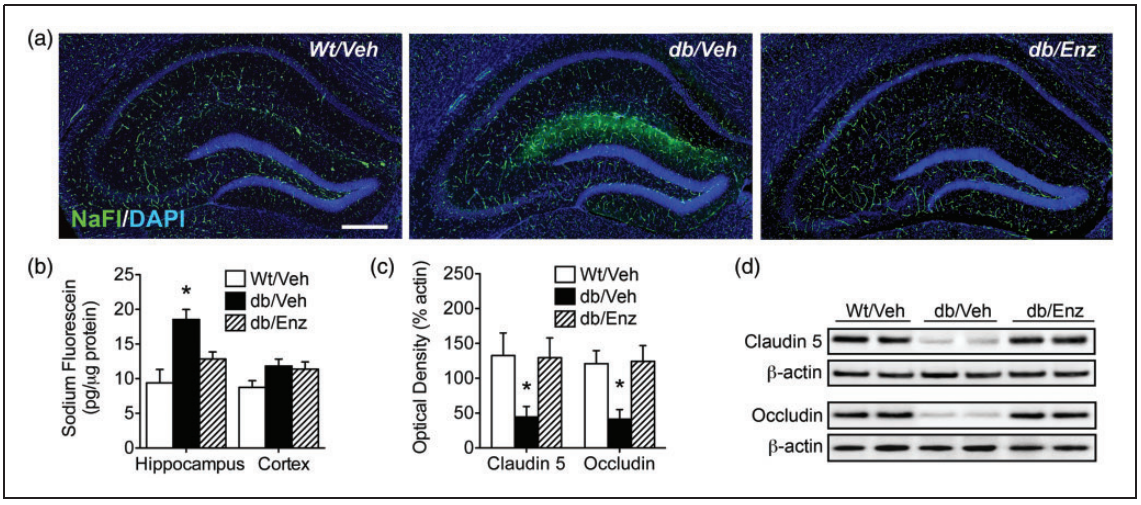

Figure 2. Genetic obesity promotes blood–brain barrier breakdown. (a) Penetration of sodium fluorescein (NaFl), a low molecular weight fluorophore that does not pass the intact BBB, is more evident on hippocampal sections from vehicle-treated db/db mice (db/Veh). Increased NaFl penetrance was observed relative to vehicle-treated Wt mice (Wt/Veh) and db/db mice administered the PKCβ inhibitor Enzastaurin (db/Enz). (b) Quantitative fluorometry in hippocampal extracts reveals that hippocampal fluorescein penetrance is significantly increased in db/Veh mice relative to db/Enz mice and Wt/Veh controls. This pattern was not evident in cortical extracts, suggestive of regional differences in vulnerability of the BBB. (c) Western blotting for the tight junction proteins claudin 5 and occludin revealed PKCβ-dependent reductions in tight junction protein expression in db/Veh mice. (d) Representative images of western blot membranes for claudin 5 and occludin. For all graphs, bars depict the mean of ($n = 6$–8) mice per group, error bars represent the sem, and asterisks (*) denote statistical significance at $p < 0.05$ following one-way ANOVA with Bonferonni's *post hoc*.

mice, but in sections from db/Enz mice, NaFl fluorescence was confined to the vasculature in a pattern similar to Wt/Veh mice (Figure 2(a)). Qualitative observations on hippocampal sections were upheld with direct quantification of NaFl in homogenates, as Enzastaurin blocked increases in hippocampal NaFl penetrance (Figure 2(b); $F_{2,18} = 5.53$, $p < 0.05$). There was no effect of genotype or PKCβ antagonism on cortical NaFl concentrations, suggesting that there may be regional heterogeneity in susceptibility to BBB breakdown.

We also quantified expression of the tight junction proteins claudin 5 and occludin, which are required for cellular adhesion between adjacent cerebrovascular endothelial cells.[18] Hippocampal tight junction protein expression was significantly reduced in db/Veh mice (Figure 2(c); for claudin 5, $F_{2,18} = 9.74$, $p < 0.01$; for occludin, $F_{2,18} = 3.79$, $p < 0.05$), and reductions were PKCβ-dependent, as db/Enz mice had levels of claudin 5 and occludin that were similar to Wt/Veh mice (Figure 2(d)). This pattern of cellular and functional alterations suggests that db/db mice exhibit PKCβ-mediated BBB breakdown.

Reinstatement of BBB integrity normalizes hippocampus-dependent memory

To examine the behavioral consequences of BBB breakdown, we measured hippocampus-dependent memory in Wt/Veh, db/Veh, and db/Enz mice. Spatial recognition memory was significantly impaired in db/Veh mice, based on reduced alternation during testing in the Y-maze ($F_{2,24} = 9.81$, $p < 0.01$; Figure 3(a)). Deficits in spatial memory were not observed in db/Enz mice, which performed similarly to Wt/Veh mice (*post hoc* *t*-tests with Bonferroni's correction: $t_{15} = 1.14$, ns). Mice were also tested in the novel object recognition paradigm, where db/Veh mice showed less preference for the novel object at the 0.5 h and 2 h post-training intervals ($F_{2,24} = 6.23$, $p < 0.05$; Figure 3(b)). Enzastaurin treatment normalized object recognition, based on comparable preference for the novel object in db/Enz and Wt/Veh mice (*post hoc* *t*-tests with Bonferroni's correction: $t_{15} = 0.37$, ns). All experimental groups spent similar total time exploring the objects (novel + familiar), indicating that changes in novel object preference are not explained by differences in motor activity or anxiety (Figure 3(b)). Taken together, these results suggest that re-establishing BBB integrity prevents memory deficits in genetic obesity and diabetes.

BBB breakdown impairs hippocampal synaptic plasticity

To determine whether pharmacological rescue of the BBB attenuates deficits in hippocampal plasticity, we recorded long-term potentiation (LTP) in slice

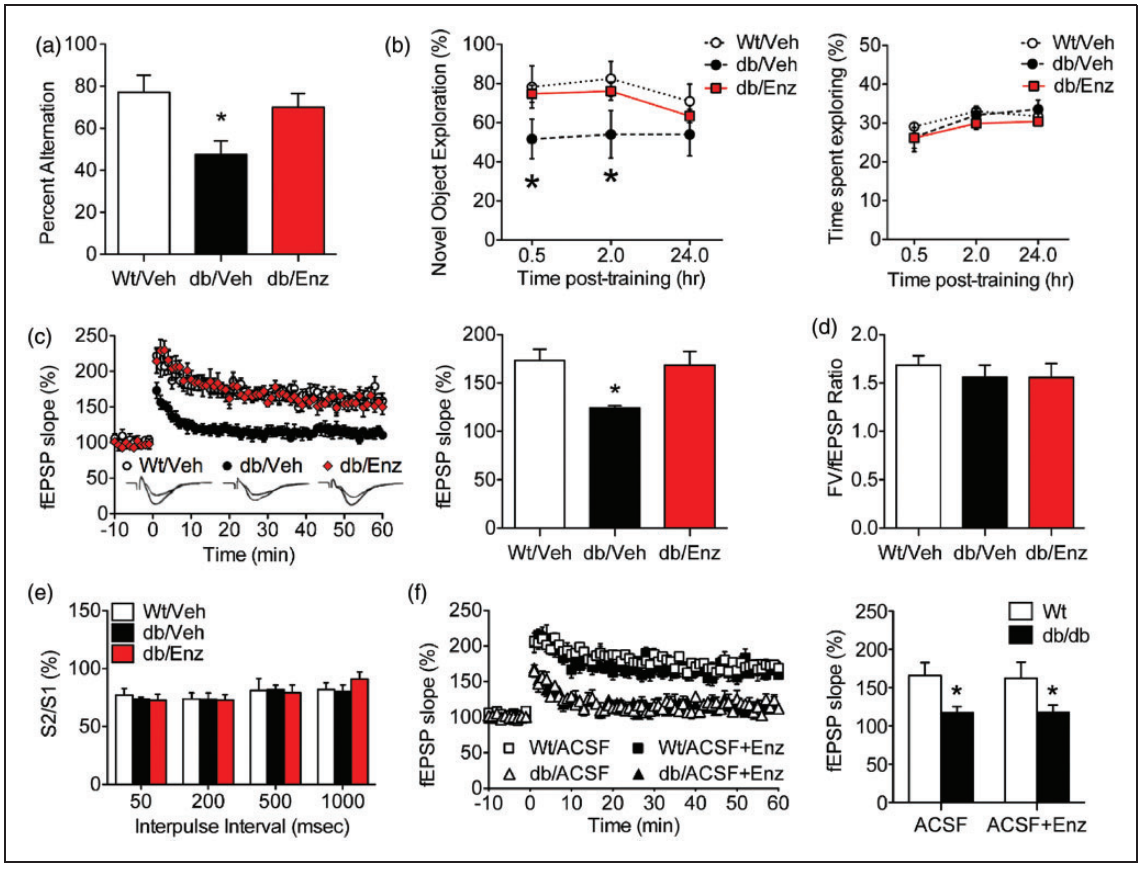

Figure 3. Pharmacological reinstatement of BBB integrity restores hippocampus-dependent memory and long-term potentiation. (a) Spatial recognition memory in the Y-maze is impaired in vehicle-treated db/db mice (db/Veh), but is normalized with Enzastaurin treatment (db/Enz). (b) Novel object recognition memory (left panel) is reduced in db/Veh mice and restored in db/Enz mice. There were no effects of genotype or Enzastaurin treatment on the total time spent exploring in each trial (right panel). (c) Reinstatement of BBB integrity in db/Enz mice rescues long-term potentiation at medial perforant path synapses on dentate gyrus granule neurons in hippocampal slices (left panel). db/Veh mice exhibit smaller increases in the slope of the field excitatory postsynaptic potential (fEPSP) during minutes 50–60 of recording (right panel), but db/Enz mice are indistinguishable from Wt mice. (d) The ratio of the presynaptic fiber volley (FV) and the postsynaptic fEPSP slope across a range of stimulation intensities was not influenced by genotype or Enzastaurin treatment. (e) Quantification of reductions in fEPSP slope after sequential stimuli (S1, S2) revealed no differences in presynaptic paired-pulse depression. (f) Direct application of the PKCβ inhibitor Enzastaurin had no effect on LTP deficits in hippocampal slices from db/db mice (left panel). PKCβ antagonism also did not influence plasticity in Wt slices (right panel). For all graphs, the height of bars or symbols depicts the average of ($n = 9$–11) mice per condition (a, b), or ($n = 12$–16) slices from mice in each condition (c–f). Error bars represent the SEM and asterisks (*) denote statistical significance at $p < 0.05$ following one-way ANOVA (a-e) or two-way ANOVA (f) with Bonferonni's post hoc.

preparations from Wt/Veh, db/Veh, or db/Enz mice. Recordings were made at medial perforant path (mPP) inputs to the hippocampal dentate gyrus, which were identified anatomically by their location in the middle molecular layer, and functionally by the presence of presynaptic paired-pulse depression (PPD).[33] Consistent with previous reports,[4,5,30,41] slices from vehicle-treated db/db mice exhibit impaired LTP relative to slices from Wt mice (Figure 3(c); $F_{2,22} = 8.51$, $p < 0.01$). Enzastaurin treatment eliminated LTP deficits in slices from db/db mice, indicating that reinstatement of BBB integrity normalizes synaptic plasticity (Figure 3(c); *post hoc t*-tests with Bonferroni's correction: $t_{15} = 0.48$, ns; Figure 6(d)). Analysis of the input–output ratio revealed no differences between groups ($F_{2,22} = 0.24$, ns; Figure 3(d)), and PPD magnitude was unchanged ($F_{2,22} = 0.68$, ns; Figure 3(e)), implying that there may be a postsynaptic mechanism for synaptic deficits following obesity-induced BBB leakiness.

PKCβ inhibition prevented BBB breakdown in db/db mice, but PKCβ is also expressed in neurons and has been linked with changes in memory.[42] To determine whether LTP reinstatement in db/Enz mice was a direct effect of PKCβ inhibition, hippocampal slices from untreated Wt or db/db mice were pre-incubated with Enzastaurin (1 μM) for 30 min before recording, with

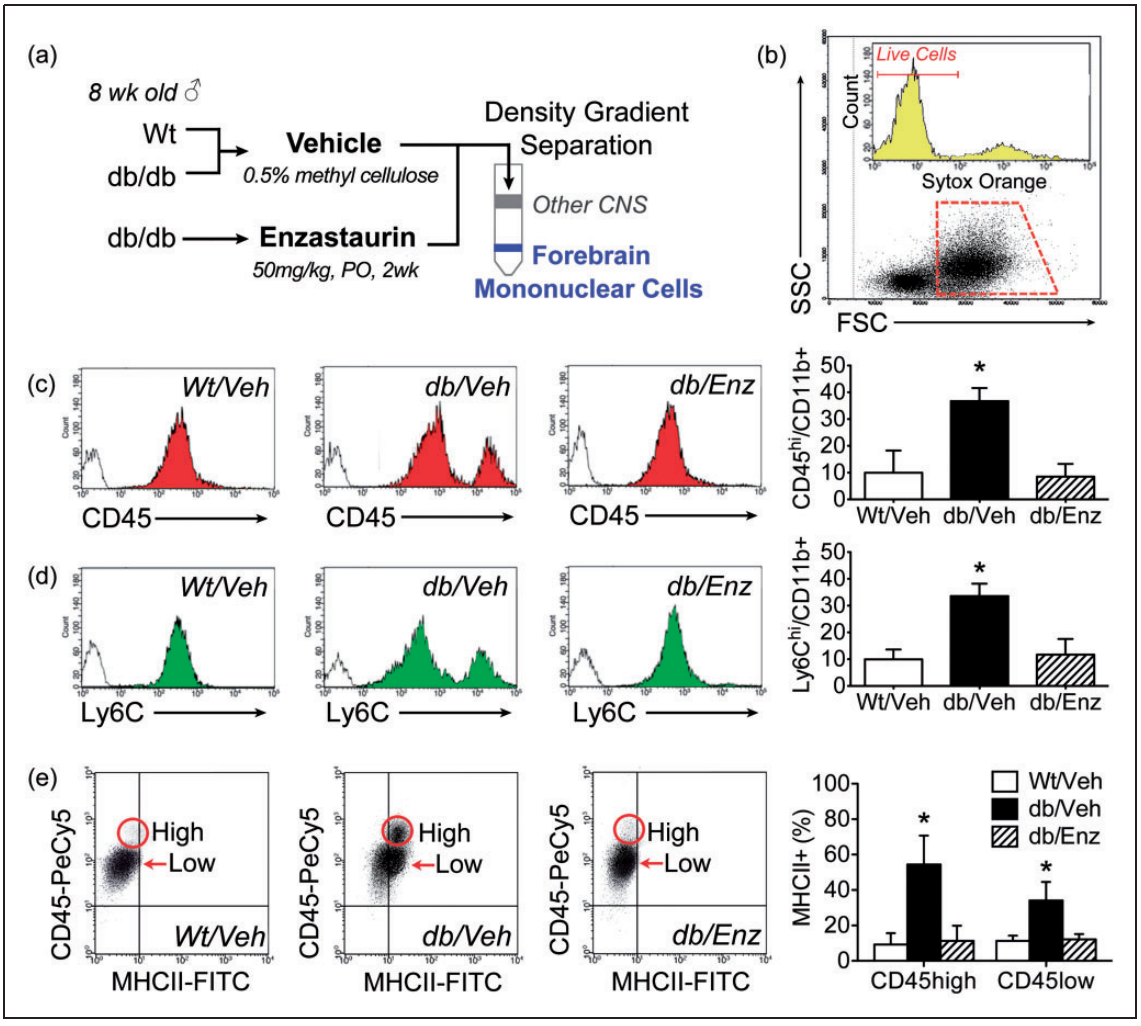

Figure 4. Blood–brain barrier breakdown promotes macrophage infiltration and classical activation in resident microglia from db/db mice. (a) Experimental timeline for Enzastaurin treatment and isolation of forebrain mononuclear cells (FMCs). (b) Cells were gated on forward and side scatter (FSC, SSC) and nonviable cells were excluded using the dead cell marker Sytox Orange. (c) Analysis of CD45hi macrophages and CD45low microglia within the population of CD11b+ cells reveals macrophage infiltration in db/Veh mice. Increases in CD45hi/CD11b+ cells were not detected in db/db mice treated with Enzastaurin (db/Enz). (d) Fluorescence intensity for the monocyte marker Ly6C also distinguishes between brain-penetrant macrophages (Ly6Chi) and resident microglia (Ly6Clow). Accumulation of Ly6Chi/CD11b + macrophages in db/Veh mice was eliminated by Enzastaurin treatment. For all histograms, filled regions represent labeling with fluorescence-conjugated antibodies and empty regions show fluorescence with isotype control. (e) Scatterplots show representative distributions of CD45hi macrophages and CD45low microglia that express the classical activation marker MHCII. Graph (far right) shows coordinated induction of MHCII in microglia and macrophages from db/Veh mice that is reversed by Enzastaurin. For all graphs, bar height shows the average of ($n = 8$) mice per group, error bars represent the SEM, and asterisks (*) denote statistical significance at $p < 0.05$ following one-way ANOVA with Bonferonni's *post hoc*.

continuous bath application throughout the experiment. This approach revealed that direct inhibition of PKCβ had no effect on LTP in slices from db/db or Wt mice (Figure 3(f); for the main effect of Enzastaurin, $F_{1,26} = 0.78$, ns). These observations are consistent with the premise that PKCβ inhibition reinstates hippocampal synaptic plasticity via indirect modulation of BBB permeability.

Blood–brain barrier breakdown enables macrophage infiltration in diabetes

To determine if BBB breakdown promotes macrophage infiltration in db/db mice, we isolated forebrain mononuclear cells from db/Veh, db/Enz, and Wt/Veh mice and used flow cytometry to identify microglia and brain-penetrant macrophages (Figure 4(a)). Freshly

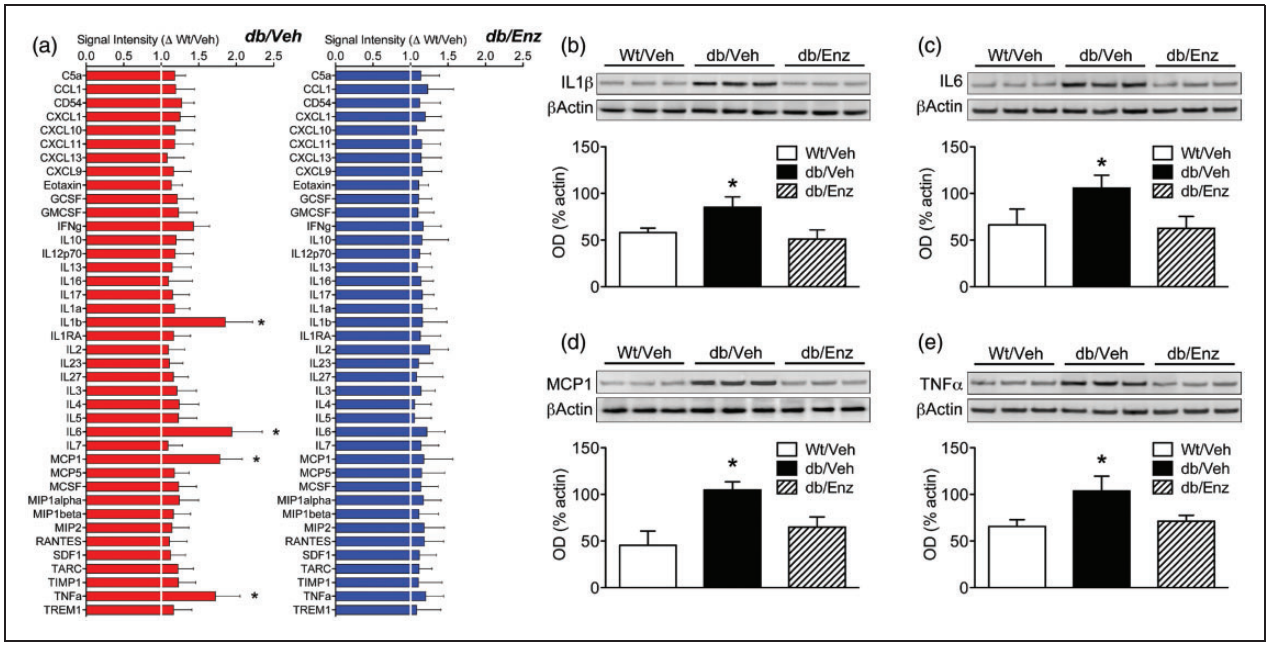

Figure 5. Induction of pro-inflammatory cytokines in brain-penetrant macrophages and resident microglia is eliminated by reinstating BBB integrity. (a) Protein array analysis of conditioned media from forebrain mononuclear cells (FMCs) isolated from vehicle-treated db/db and Wt mice (db/Veh, Wt/Veh) and from db/db mice administered the PKCβ inhibitor Enzastaurin (db/Enz). Graphs represent data from db/Veh and db/Enz cells, with each target normalized to the corresponding mean intensity in samples from Wt/Veh cells. FMCs from db/Veh mice released significantly more interleukin 1β (IL1β), interleukin 6 (IL6), monocyte chemoattractant protein 1 (MCP1) and tumor necrosis factor-α (TNFα), but induction of these pro-inflammatory cytokines was not detected in cells from db/Enz mice. (b) Quantification of interleukin 1β (IL1β) by western blotting in cell lysates revealed increased IL1β in db/Veh cells, but not in db/Enz cells. (c) Reinstatement of BBB integrity in db/Enz mice reduced levels of IL6 in cell lysates. (d) FMCs from db/Veh mice, but not db/Enz mice, exhibit increases in MCP1 protein. (e) PKCβ antagonism prevents increases in TNFα in cell lysates from db/db mice. For all graphs, bar height depicts the mean fold change from Wt/Veh (A) or the group mean (B-E) from ($n = 6$) mice per condition. Error bars represent the SEM and asterisks (*) denote statistical significance at $p < 0.05$ following one-way ANOVA with Bonferonni's *post hoc*.

isolated forebrain mononuclear cells (FMCs) were first gated on forward and side scatter (FSC, SSC; Figure 4(b)). This strategy routinely revealed a population of SSClow events with the morphological and cytological characteristics shared by macrophages and microglia. Cells that were positive for the dead cell marker Sytox Orange were then gated out and excluded (Figure 4(b)). The proportion of nonviable cells was routinely <10% and did not differ between Wt/Veh, db/Veh, or db/Enz mice (nonviable cells as percent of SSClow gated population; mean ± SEM, Wt/Veh = 8.6 ± 0.3, db/Veh = 9.2 ± 0.5, db/Enz = 9.3 ± 0.4). After applying this gating strategy, analysis of CD45hi and CD45low cells within the population of cells expressing the macrophage and microglial marker CD11b revealed that db/Veh mice exhibit significant increases CD45hi/CD11b + cells, relative to all other groups (Figure 4(c); $F_{2,18} = 9.31$, $p < 0.01$). Accumulation of CD45hi/CD11b+ macrophages did not occur in db/Enz mice (Figure 4(c); *post hoc* Bonferonni-corrected *t*-test compared with Wt/Veh, ns). A similar pattern was detected using antibodies against the myeloid lineage marker Ly6C, which is also expressed at higher levels in peripheral monocytes relative to brain-resident microglia.[43] db/db mice exhibit significant increases in Ly6Chi/CD11b+ cells that were eliminated by Enzastaurin treatment (Figure 4(d); $F_{2,19} = 6.47$, $p < 0.01$), consistent with the idea that re-establishing BBB integrity prevents macrophage infiltration in diabetes and obesity.

Parallel activation of microglia and brain-penetrant macrophages in diabetes

To investigate relationships between BBB breakdown, macrophage infiltration, and microglial activation, FMCs from db/Veh, db/Enz, and Wt/Veh mice were labeled with antibodies against CD45 and the classical activation marker MHCII.[43,44] Analysis of MHCII induction in CD45hi and CD45low cells revealed parallel activation of microglia and macrophages in db/Veh mice (Figure 4(e)). MHCII expression was likely attributable to BBB breakdown, as Enzastaurin treatment eliminated MHCII induction in CD45+ cells

from db/Enz mice ($F_{2,18} = 3.87$, $p < 0.05$, Figure 4(b)). Because CD45hi cells made up only a small proportion (<10%) of gated events in Wt/Veh and db/Enz mice, it was not possible to accurately measure MHCII expression in CD45hi cells in these conditions. The primary conclusion from these experiments is that both CD45low microglia and CD45hi macrophages are activated by BBB breakdown in obesity and diabetes.

To investigate the relationships between macrophage infiltration and cytokine release in obesity and diabetes, FMCs were isolated from additional groups of Wt/Veh, db/Veh, and db/Enz mice. Plated cells were maintained in serum-free media for 2 h and conditioned media samples were collected for protein array profiling. This approach revealed significant elevations in interleukin 1β (IL1β), interleukin 6 (IL6), monocyte chemoattractant protein 1 (MCP1), and tumor necrosis factor-α (TNFα) in media samples from db/Veh cells (Figure 5(a)). Induction of inflammatory cytokines did not occur in conditioned media from db/Enz cells (Figure 5(a)), suggesting that macrophage infiltration promotes inflammatory cytokine release in FMCs from db/db mice.

The changes in cytokines detected in conditioned media were further validated by western blotting in cell lysates. Consistent with the protein array data, FMCs from db/Veh mice expressed significantly higher levels of IL1β, IL6, MCP1, and TNFα (Figure 5(b) to (e); for IL1β, $F_{2,18} = 7.64$, $p < 0.01$; for IL6, $F_{2,18} = 6.73$, $p < 0.02$; for MCP1, $F_{2,18} = 8.54$, $p < 0.01$; for TNFa, $F_{2,18} = 9.32$, $p < 0.01$). Expression of these targets in db/Enz cell lysates was identical to expression in Wt/Veh cells (Figure 5(b) to (e)), consistent with the idea that infiltrating macrophages are required for inflammatory cytokine induction in diabetes and obesity.

Obesity promotes macrophage transmigration by increasing IL1β

Macrophage infiltration into the brain with diabetes and obesity could be a passive consequence of BBB breakdown, or could be attributable to BBB breakdown and attraction by a chemokine gradient. To examine these scenarios, FMCs from untreated Wt or db/db mice were plated below peritoneal macrophages in Boyden chamber inserts. Because FMCs required serum supplementation in maintenance media during the overnight exposure, we initially conducted control experiments to examine transmigration in the absence of FMCs (Supplementary Figure 1). Peritoneal macrophages from Wt and db/db mice exhibit similar transmigration in response to media supplemented with 5% fetal bovine serum (FBS; Supplementary Figure 1A). Unstimulated migration towards serum-free media was also comparable in peritoneal macrophages from either genotype (Supplementary Figure 1B). These control conditions were run with every experiment and were used to generate a migration index, with peritoneal macrophage migration towards media with 5% FBS subtracted from migration in response to FMCs in media with 5% FBS. This value was then expressed relative to negative control wells without cells on a per-sample basis.

Peritoneal macrophages from db/db mice exhibit increases in migration, but only when plated above FMCs isolated from another db/db mouse (Figure 6(a) and (b); $F_{1,28} = 3.71$, $p < 0.05$). Wt peritoneal macrophages exhibit similar migration when plated above FMCs from another Wt or a db/db mouse, suggesting that both the central and peripheral effects of diabetes and obesity were required to promote migration across the synthetic barrier. When FMCs from Wt or db/db mice were plated below inserts containing only serum-free media, there was no evidence of detachment from the wells and adherence to the bottom of the insert (Supplementary Figure 1C and D). Taken together with results from the flow cytometry experiments (Figure 4(c) and (d)), the transmigration results indicate that signaling between peripheral macrophages and FMCs might be facilitated by BBB breakdown in obesity. A permissive role for BBB leakiness in macrophage infiltration is possible based on reductions in brain-penetrant macrophages following Enzastaurin treatment in db/db mice (Figure 4(e)). However, the flow cytometry results do not rule out the potential direct effects of PKCβ inhibition on macrophage homing and migration.

To investigate the consequences of PKCβ inhibition for transmigration and attraction between macrophages and FMCs, we treated peritoneal macrophages with Enzastaurin (1 μM) and plated them above FMCs from Wt or db/db mice (Supplementary Figure 2A). If the effects of systemic Enzastaurin in db/db mice were mediated by PKCβ inhibition on macrophages, then direct application of Enzastaurin would be expected to block attraction between db/db peritoneal macrophages and db/db FMCs. These experiments revealed comparable increases in migration in Enzastaurin-treated and untreated db/db macrophages plated above db/db FMCs ($F_{1,28} = 6.34$, $p < 0.01$). There was also no effect of PKCβ inhibition on migration in Wt macrophages plated above Wt FMCs (Supplementary Figure 2B). These results indicate that reductions in macrophage infiltration in db/Enz mice are not explained by direct effects of PKCβ inhibition on peripheral macrophages.

To investigate whether chemokines identified in the protein arrays mediate attraction between macrophages and FMCs, we examined migration using a similar design in the presence of inhibitors and antagonists against IL1, IL6, MCP1, and TNFα. Incubation with

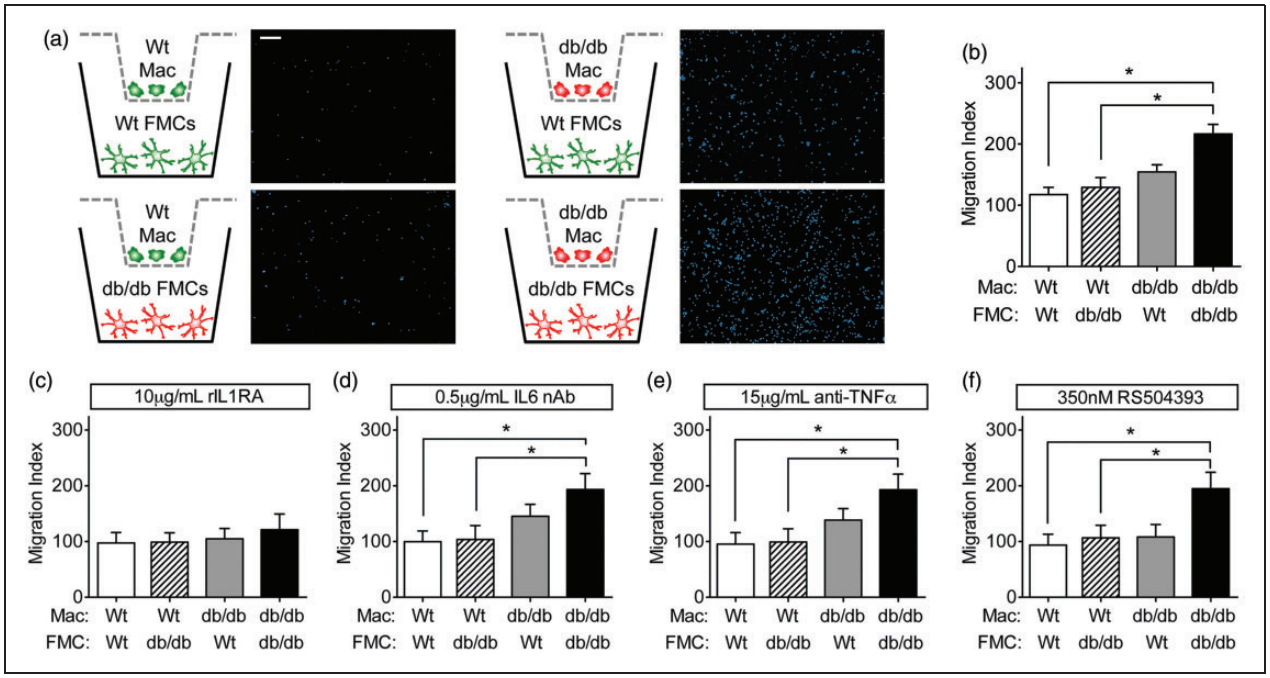

Figure 6. Interleukin 1 mediates attraction between peripheral macrophages and forebrain mononuclear cells in genetic obesity. (a) Schematic diagram represents experimental design for analysis of migration in peritoneal macrophages (Mac) and forebrain mononuclear cells (FMCs). Micrographs to the right of each schematic show representative images of macrophage transmigration in each condition visualized with the nuclear marker DAPI. Scalebar = 100 microns. (b) Transmigration is selectively enhanced when peritoneal macrophages from db/db mice are plated above FMCs from another db/db mouse. (c) Incubation with recombinant interleukin 1 receptor antagonist (rIL1RA) prevents increases in transmigration. (d) Incubation with a neutralizing antibody against interleukin 6 (IL6 nAb) does not influence transmigration. (e) Antibody-based inhibition of tumor necrosis factor alpha (anti-TNFa) does not affect transmigration. (f) The monocyte chemoattractant protein 1 (MCP1) receptor antagonist RS504393 does not prevent increases in transmigration in db/db macrophages plated above db/db FMCs. For all graphs, bar height shows the average of ($n = 8$–11) mice per condition, error bars represent the SEM, and asterisks (*) denote statistical significance at $p < 0.05$ following 2×2 ANOVA.

recombinant interleukin 1 receptor antagonist (IL1RA) prevented increases in migration when db/db peritoneal macrophages were plated above db/db FMCs (Figure 6(c); $F_{1,28} = 0.51$, ns). By contrast, neutralizing antibodies against IL6 had no effect on migration between db/db peritoneal macrophages and db/db FMCs, indicating that attraction between these cell types was IL6-independent (Figure 6(d); $F_{1,26} = 7.98$, $p < 0.01$). The TNFα-binding antibody adalimumab also did not influence migration between db/db macrophages and db/db FMCs (Figure 6(e); $F_{1,27} = 8.52$, $p < 0.01$), suggesting that communication between these cell types does not directly involve TNFα. Increases in migration between db/db macrophages and db/db FMCs were also detected in the presence of the MCP1 receptor antagonist RS504393 (Figure 6(f); $F_{1,24} = 4.64$, $p < 0.05$). None of the antibodies or antagonists altered migration between Wt peritoneal macrophages and FMCs from either genotype, which suggests that IL1 plays a central role in CNS macrophage infiltration in obesity and diabetes.

Discussion

These studies represent the first mechanistic evidence for a relationship between blood–brain barrier breakdown, neuroinflammation, and cognitive deficits in type 2 diabetes and obesity. Protein kinase Cβ antagonism prevented BBB breakdown and normalized hippocampus-dependent memory and synaptic plasticity in db/db mice. Reinstating BBB integrity also prevented accumulation of brain-penetrant macrophages and eliminated the induction of classical activation markers in forebrain mononuclear cells in db/db mice, with commensurate reductions in inflammatory cytokines. Peritoneal macrophages from db/db mice exhibit increased migration towards db/db forebrain mononuclear cells, and attraction between these cell types was IL1-dependent. Taken together, these findings indicate that BBB leakiness facilitates hippocampal cytokine induction, macrophage infiltration, and cognitive impairment in diabetes and obesity.

db/db mice exhibit early-onset hyperglycemia and insulin resistance, as well as severe obesity.[39] The findings

in this report suggest that PKCβ-mediated BBB breakdown impairs hippocampal function in obesity and diabetes by exposing the CNS to circulating immune cells and inflammatory cytokines. However, questions remain surrounding the mechanisms that initiate BBB breakdown and macrophage infiltration in these experiments. On one hand, hyperglycemia increases retinal cerebrovascular permeability by activating PKCβ.[27,45,46] This robust and widely replicated finding led to initiation of clinical trials to determine whether ruboxistaurin, a related PKCβ inhibitor, might treat or delay the progression of diabetic retinopathy in humans.[47] On the other hand, nondiabetic obesity promotes cerebrovascular inflammation, leading to vascular adherence by circulating immune cells.[48,49] Taken together, previous work in this area suggests that changes in cerebrovascular permeability and infiltration of peripheral immune cells may be mediated by dissociable mechanisms in diabetes and obesity. Future studies will address this possibility using cell type-specific manipulation of endothelial cells in mice with obesity, or comorbid obesity and diabetes.

Microglial activation in hypothalamic nuclei is an increasingly recognized response to metabolic dysfunction in diabetes and obesity,[2] and systemic PKCβ ntagonism could potentially attenuate BBB breakdown and local inflammation in the hypothalamus, as well as the hippocampus. However, we observed no reductions in body weight or changes in insulin sensitivity in db/db mice treated with Enzastaurin, suggesting that the effects of PKCβ inhibition on metabolism were limited if present. The time course and regional extent of BBB breakdown in diabetes has yet to be characterized, and the temporal onset of neuroinflammation in different brain regions similarly remains to be determined. These gaps in knowledge constrain interpretation of the data in this report with respect to extrahippocampal regulation of BBB integrity and microglial activation.

Under normal physiological conditions, hippocampal neurons are protected by the BBB, but a number of brain regions, including the circumventricular organ and subfornical organ, lack a functional barrier[50] and would therefore be exposed to the PKCβ inhibitor. While PKCβ is involved in a range of cellular functions, the relative efficacy of PKCβ antagonism in different cell types has yet to be determined. The lack of data on neuronal responses to PKCβ antagonism in the subfornical and circumventricular regions that lack a functional BBB limits our ability to speculate regarding the potential direct effects of Enzastaurin treatment on these brain areas. However, direct application of Enzastaurin in hippocampal slices did not alter LTP deficits in db/db mice, suggesting that systemic PKCβ antagonism might restore plasticity indirectly by normalizing BBB integrity.

Activation of cytosolic PKCβ promotes membrane translocation and conformational changes that expose the ATP-binding pocket.[51] Enzastaurin competes with ATP for binding to catalytic sites required for PKCβ kinase activity.[52,53] The dose, duration, and route of administration chosen for experiments in the current report were based on previous studies demonstrating restoration of BBB integrity in experimental autoimmune encephalitis after Enzastaurin treatment.[26] *In vitro* exposure to Enzastaurin upregulates tight junction proteins in murine cerebrovascular endothelial cells without altering basal or stimulated cytokine release.[26] Although the data in the current report do not conclusively demonstrate that systemic PKCβ inhibition rescues hippocampal function by re-establishing BBB integrity, LTP deficits in db/db mice were unaffected by direct application of Enzastaurin. This result suggests that restoration of synaptic plasticity and cognition with *in vivo* administration is unlikely to be centrally mediated. Moreover, while we cannot rule out the possibility that reductions in hippocampal macrophage infiltration in db/Enz mice might be mediated by extra-cerebrovascular effects of PKCβ inhibition, there was no direct effect of Enzastaurin on attraction between peritoneal macrophages and forebrain mononuclear cells from db/db mice in these experiments. These results are consistent with previous work in models of infection, which suggest that off-target effects on the transmigration of circulating immune cells are minimal following systemic Enzastaurin treatment.[26] When interpreted in the context of previous work demonstrating reinstatement of cerebrovascular barrier function following PKCβ inhibition in vivo and in vitro,[26] the results of the current report strongly suggest that rescuing the BBB prevents neuroinflammation and cognitive dysfunction in obesity and diabetes.

There are a number of scenarios that could contribute to brain macrophage infiltration in obesity and diabetes. Barrier breakdown alone could be sufficient, or may work in concert with a chemokine gradient from resident microglia that promotes macrophage infiltration. Alternatively or in addition, the severity of barrier breakdown might increase over time, with initial small increases in BBB permeability allowing circulating factors to enter the brain and activate microglia, causing their release of chemokines that attract macrophages across the progressively leakier BBB. These scenarios remain speculative at present, and future cell-type-specific manipulations will be necessary to determine which mechanism(s) drive brain inflammation and cognitive impairment in type 2 diabetes and obesity. In human studies, body mass index in middle age predicted subsequent BBB breakdown, based on analysis of cerebrospinal fluid and serum albumin levels.[19] The gradual erosion of the BBB in human obesity has

important clinical implications, as the CNS bioavailability of drugs may be increased with obesity-induced BBB breakdown. Because the cerebral vasculature is a more accessible therapeutic target than the CNS, understanding the role of BBB breakdown in obesity-induced memory deficits could identify strategies for the treatment and prevention of cognitive impairment in obese individuals.

Funding

The author(s) disclosed receipt of the following financial support for the research, authorship, and/or publication of this article: These studies were supported by a grant from the National Institutes of Health to AMS (grant no. K01DK100616).

Declaration of conflicting interests

The author(s) declared no potential conflicts of interest with respect to the research, authorship, and/or publication of this article.

Authors' contributions

AMS and BB designed the research; AMS, SH, AD, and XY performed the research; and all authors provided input on the manuscript.

Supplementary material

Supplementary material for this paper can be found at http://jcbfm.sagepub.com/content/by/supplemental-data

References

1. Kanneganti TD and Dixit VD. Immunological complications of obesity. *Nat Immunol* 2012; 13: 707–712.
2. Kälin S, Heppner FL, Bechmann I, et al. Hypothalamic innate immune reaction in obesity. *Nat Rev Endocrinol* 2015; 11: 339–351.
3. Stranahan AM. Models and mechanisms for hippocampal dysfunction in obesity and diabetes. *Neuroscience* 2015; 309: 125–139.
4. Erion JR, Wosiski-Kuhn M, Dey A, et al. Obesity elicits interleukin 1-mediated deficits in hippocampal synaptic plasticity. *J Neurosci* 2014; 34: 2618–2631.
5. Hao S, Dey A, Yu X, et al. Dietary obesity reversibly induces synaptic stripping by microglia and impairs hippocampal plasticity. *Brain Behav Immun* 2016; 51: 230–239.
6. Sobesky JL, Barrientos RM, De May HS, et al. High-fat diet consumption disrupts memory and primes elevations in hippocampal IL-1β, an effect that can be prevented with dietary reversal or IL-1 receptor antagonism. *Brain Behav Immun* 2014; 42: 22–32.
7. Burke SN and Barnes CA. Senescent synapses and hippocampal circuit dynamics. *Trends Neurosci* 2010; 33: 153–161.
8. Fotuhi M, Do D and Jack C. Modifiable factors that alter the size of the hippocampus with ageing. *Nat Rev Neurol* 2012; 8: 189–202.
9. Elias MF, Elias PK, Sullivan LM, et al. Obesity, diabetes and cognitive deficit: the Framingham heart study. *Neurobiol Aging* 2005; 26: 11–16.
10. Xu WL, Atti AR, Gatz M, et al. Midlife overweight and obesity increase late-life dementia risk: a population-based twin study. *Neurology* 2011; 76: 1568–1574.
11. Ho AJ, Raji CA, Becker JT, et al. Obesity is linked with lower brain volume in 700 AD and MCI patients. *Neurobiol Aging* 2010; 31: 1326–1339.
12. Whitmer RA, Gustafson DR, Barrett-Connor E, et al. Central obesity and increased risk of dementia more than three decades later. *Neurology* 2008; 71: 1057–1064.
13. Convit A, Wolf OT, Tarshish C, et al. Reduced glucose tolerance is associated with poor memory performance and hippocampal atrophy among normal elderly. *Proc Natl Acad Sci USA* 2003; 100: 2019–2022.
14. Xu W, Caracciolo B, Wang HX, et al. Accelerated progression from mild cognitive impairment to dementia in people with diabetes. *Diabetes* 2010; 59: 2928–2935.
15. Ott A, Stolk RP, Hofman A, et al. Association of diabetes mellitus and dementia: the Rotterdam Study. *Diabetologia* 1996; 39: 1392–1397.
16. Zhao Z, Nelson AR, Betsholtz C, et al. Establishment and dysfunction of the blood–brain barrier. *Cell* 2015; 163: 1064–1078.
17. Abbott NJ, Rönnbäck L and Hansson E. Astrocyte-endothelial interactions at the blood–brain barrier. *Nat Rev Neurosci* 2006; 7: 41–53.
18. Wolburg H and Lippoldt A. Tight junctions of the blood–brain barrier: development, composition and regulation. *Vasc Pharmacol* 2002; 38: 323–337.
19. Gustafson D, Karlsson C, Skoog I, et al. Mid-life adiposity factors relate to blood–brain barrier integrity in late life. *J Intern Med* 2007; 262: 643–650.
20. Montagne A, Barnes SR, Sweeney MD, et al. Blood–brain barrier breakdown in the aging human hippocampus. *Neuron* 2015; 85: 296–302.
21. Zlokovic BV. Neurovascular mechanisms of Alzheimer's neurodegeneration. *Trends Neurosci* 2005; 28: 202–208.
22. Saunders NR, Ek CJ, Habgood MD, et al. Barriers in the brain: a renaissance? *Trends Neurosci* 2008; 31: 279–286.
23. Quan N. Immune-to-brain signaling: how important are the blood–brain barrier-independent pathways? *Mol Neurobiol* 2008; 37: 142–152.
24. Hanisch UK and Kettenmann H. Microglia: active sensor and versatile effector cells in the normal and pathologic brain. *Nat Neurosci* 2007; 10: 1387–1394.
25. Prinz M and Priller J. Microglia and brain macrophages in the molecular age: from origin to neuropsychiatric disease. *Nat Rev Neurosci* 2014; 15: 300–312.
26. Lanz TV, Becker S, Osswald M, et al. Protein kinase Cβ as a therapeutic target stabilizing blood–brain barrier disruption in experimental autoimmune encephalomyelitis. *Proc Natl Acad Sci U S A* 2013; 110: 14735–14740.
27. Ishii H, Jirousek MR, Koya D, et al. Amelioration of vascular dysfunctions in diabetic rats by an oral PKC beta inhibitor. *Science* 1996; 272: 728–731.
28. Kanoski SE, Zhang Y, Zheng W, et al. The effects of a high-energy diet on hippocampal function and

blood–brain barrier integrity in the rat. *J Alzheimers Dis* 2010; 21: 207–219.
29. Dey A, Hao S, Erion JR, et al. Glucocorticoid sensitization of microglia in a genetic mouse model of obesity and diabetes. *J Neuroimmunol* 2014; 269: 20–27.
30. Wosiski-Kuhn M, Erion JR, Gomez-Sanchez EP, et al. Glucocorticoid receptor activation impairs hippocampal plasticity by suppressing BDNF expression in obese mice. *Psychoneuroendocrinology* 2014; 42: 165–177.
31. Wosiski-Kuhn M and Stranahan AM. Transient increases in dendritic spine density contribute to dentate gyrus long-term potentiation. *Synapse* 2012; 66: 661–664.
32. Meng XW, Heldebrant MP, Flatten KS, et al. Protein kinase Cbeta modulates ligand-induced cell surface death receptor accumulation: a mechanistic basis for enzastaurin-death ligand synergy. *J Biol Chem* 2010; 285: 888–902.
33. Asztely F, Kokaia M, Olofsdotter K, et al. Afferent-specific modulation of short-term synaptic plasticity by neurotrophins in dentate gyrus. *Eur J Neurosci* 2000; 12: 662–669.
34. Zhang X, Goncalves R and Mosser DM. The isolation and characterization of murine macrophages. *Curr Protoc Immunol* 2008, Chap. 14:83:14.1.1–14.1.14 DOI: 10.1002/0471142735.im1401s83.
35. Distler JH, Jüngel A, Huber LC, et al. The induction of matrix metalloproteinase and cytokine expression in synovial fibroblasts stimulated with immune cell microparticles. *Proc Natl Acad Sci USA* 2005; 102: 2892–2897.
36. Furuichi K, Wada T, Iwata Y, et al. CCR2 signaling contributes to ischemia-reperfusion injury in kidney. *J Am Soc Nephrol* 2003; 14: 2503–2515.
37. Ai D, Jiang H, Westerterp M, et al. Disruption of mammalian target of rapamycin complex 1 in macrophages decreases chemokine gene expression and atherosclerosis. *Circ Res* 2014; 114: 1576–1584.
38. Ronda N, Greco D, Adorni MP, et al. Newly identified antiatherosclerotic activity of methotrexate and adalimumab: complementary effects on lipoprotein function and macrophage cholesterol metabolism. *Arthritis Rheumatol* 2015; 67: 1155–1164.
39. Hummel KP, Dickie MM and Coleman DL. Diabetes, a new mutation in the mouse. *Science* 1966; 153: 1127–1128.
40. Mima A, Ohshiro Y, Kitada M, et al. Glomerular-specific protein kinase C-β-induced insulin receptor substrate-1 dysfunction and insulin resistance in rat models of diabetes and obesity. *Kidney Int* 2011; 79: 883–896.
41. Li XL, Aou S, Oomura Y, et al. Impairment of long-term potentiation and spatial memory in leptin receptor-deficient rodents. *Neuroscience* 2002; 113: 607–615.
42. Weeber EJ, Atkins CM, Selcher JC, et al. A role for the beta isoform of protein kinase C in fear conditioning. *J Neurosci* 2000; 20: 5906–5914.
43. Wohleb ES, Powell ND, Godbout JP, et al. Stress-induced recruitment of bone marrow-derived monocytes to the brain promotes anxiety-like behavior. *J Neurosci* 2013; 33: 13820–13833.
44. Ting JP and Trowsdale J. Genetic control of MHC class II expression. *Cell* 2002; 109: S21–S33.
45. Murakami T, Frey T, Lin C, et al. Protein kinase cβ phosphorylates occludin regulating tight junction trafficking in vascular endothelial growth factor-induced permeability in vivo. *Diabetes* 2012; 61: 1573–1583.
46. Joy SV, Scates AC, Bearelly S, et al. Ruboxistaurin, a protein kinase C beta inhibitor, as an emerging treatment for diabetes microvascular complications. *Ann Pharmacother* 2005; 39: 1693–1699.
47. Aiello LP, Vignati L, Sheetz MJ, et al. Oral protein kinase c β inhibition using ruboxistaurin: efficacy, safety, and causes of vision loss among 813 patients (1,392 eyes) with diabetic retinopathy in the Protein Kinase C β Inhibitor-Diabetic Retinopathy Study and the Protein Kinase C β Inhibitor-Diabetic Retinopathy Study 2. *Retina* 2011; 31: 2084–2094.
48. Abiko T, Abiko A, Clermont AC, et al. Characterization of retinal leukostasis and hemodynamics in insulin resistance and diabetes: role of oxidants and protein kinase-C activation. *Diabetes* 2003; 52: 829–837.
49. Ip BC, Hogan AE and Nikolajczyk BS. Lymphocyte roles in metabolic dysfunction: of men and mice. *Trends Endocrinol Metab* 2015; 26: 91–100.
50. Pedersen EB, McNulty JA, Castro AJ, et al. Enriched immune-environment of blood–brain barrier deficient areas of normal adult rats. *J Neuroimmunol* 1997; 76: 117–131.
51. Newton AC. Protein kinase C: poised to signal. *Am J Physiol Endocrinol Metab* 2010; 298: E395–402.
52. Faul MM, Gillig JR, Jirousek MR, et al. Acyclic N-(azacycloalkyl)bisindolylmaleimides: isozyme selective inhibitors of PKCbeta. *Bioorg Med Chem Lett* 2003; 13: 1857–1859.
53. Podar K, Raab MS, Zhang J, et al. Targeting PKC in multiple myeloma: in vitro and in vivo effects of the novel, orally available small-molecule inhibitor enzastaurin (LY317615.HCl). *Blood* 2007; 109: 1669–1677.